turbance due to the wire. As can be seen in Fig. 2, the flow field in the plane normal to the wire support is severely disturbed by the presence of the wire. Hence, it is not surprising that a seemingly insignificant wire support can materially alter the wake shape.

A similar interference investigation was carried out for 30° included-angle cones at $1.6 < M < 4.7$. At $M < 2$, there did not appear to be a strong effect of the support wire (about 2% of the cone diameter) on the shape of the separation region for the high Reynolds number condition (Fig. 3a). But at the lower Reynolds numbers ($<2 \times 10^5$), when the wake was definitely laminar to beyond the neck region, the presence of the wire support did decrease the distance of the wake neck to the model. However, at $M > 2$, the effect of the wire support was quite pronounced at high as well as at low Reynolds numbers; a typical example at $M = 4.7$ being shown in Fig. 3b. As in the case of the sphere, the presence of the wire support moved the wake neck toward the cone base. Investigations at $M = 9$ in the Jet Propulsion Laboratory 21-in. hypersonic wind tunnel show that the normally convergent wakes of free-flight cone models become divergent when the $1\frac{1}{2}$-in.-diam models are supported on a single traverse 0.024-in.-diam wire.

Sketchy experimental evidence indicates that when the model boundary layer is turbulent, the presence of a wire support does not materially alter the shape of the wake separation region. This has been observed at $M = 4$ for blunted cones of nose radius to base radius ratios of 0.05 and 0.50. At $M = 1.6$ and $M = 2$, when the wire support did not alter the wake separation region of the 30° apex-angle cone, the shape of the separation region of these models was the same whether or not the model boundary layer was laminar or turbulent (obtained by tripping the boundary layer).

A further word of caution pertains to outside disturbances in the wake which may propagate forward to the model base region. Even for free-flight models, an object in the wake or a shock-wave (reflected model bow shock or from some other source such as a sabot) intersecting the wake, not far enough downstream of the model, may alter the base region flow field. Drag coefficients of spheres were measured during the work described in Ref. 1. At $M = 1.3$ when a $1\frac{1}{2}$-in.-diam sphere was used in the Jet Propulsion Laboratory 20-in. supersonic wind tunnel, the bow shock intersected the wake about 2 diam downstream from the base. This interference caused a 4% decrease in the measured drag coefficient relative to ballistic range data. When the bow shock intersected the wake five or more diameters from the base, the measured drag coefficients were within 1% of ballistic range data. A similar decrease in the drag coefficient has been observed on sting-mounted spheres (Ref. 3, Appendix) when the bow shock wave intersects the wake too near the model.

From the support-wire wake-interference studies, it has been shown that such a manner of supporting models is likely to cause incorrect base flow conditions. Even if it is suspected that a wire support, or some other seemingly negligible support, will not alter the model base flow under the particular conditions being investigated, such should be demonstrated to be the case and not just be assumed. Also, any outside disturbance in the wake must be kept far enough downstream in order that it does not propagate forward to the model and alter the base region flow field.

References

[1] Dayman, B., Jr., "Simplified free-flight testing in a conventional wind tunnel," TR 32-346, Jet Propulsion Lab., Pasadena, Calif. (October 1962).

[2] Dayman, B., Jr., "Optical free-flight wake studies," TR 32-364, Jet Propulsion Lab., Pasadena, Calif. (November 1, 1962).

[3] Dayman, B., Jr., "Prediction of blocking in the supersonic wind tunnel during an attempted start," External Publ. 669, Jet Propulsion Lab., Pasadena, Calif. (June 1959).

Scatter of Observed Buckling Loads of Pressurized Shells

F. W. Niedenfuhr*
The Ohio State University, Columbus, Ohio

Individual experimenters who have determined the buckling load of shells with external pressure generally have shown self-consistent results, but when a large number of experiments are compared it is difficult to discern even trends in the data. Evidence of the state of affairs can be found in the graphical displays of experimental data given in Refs. 1 and 2. Reference 1 also contains experimental data that indicate the general validity of the Biezeno solution for the critical load of a spherical cap compressed by a concentrated force. The difference in the correlation between theory and experiment in the two cases is marked, even to the untrained eye. Recent experiments reported in Ref. 3 show that the classical buckling load can be reached very nearly on axially loaded cylinders. However, according to Refs. 3 and 4, lower buckling loads can be obtained by using shells with artificially induced imperfections.

The presence of minute imperfections in shells has been postulated to explain the discrepancy between theoretical and experimental results, and nonlinear theory has helped to clarify the situation, since it now is known that the instability is of the *transitional* rather than of the *bifurcation* type. That is, the load deformation curve is of the general shape shown in Fig. 1. The supposed presence of vanishingly small imperfections points to a buckling load of the magnitude indicated by A or C of Fig. 1 but does not explain fully how the shell equilibrium configuration can jump from A to C. Furthermore, imperfections (if actually present) do not seem to affect shells loaded by concentrated forces, for the agreement between theory and observation is good there, as previously mentioned.

These considerations led the writer to speculate on other possible explanations of the wide scatter of experimental values. One idea that appears to hold some promise is the following: *a mechanical system that is loaded by nonconservative generalized forces may buckle dynamically as well as statically.*

The concept of dynamic instability of compressed columns was introduced by Max Beck,[5] who showed that a finite dynamic buckling load existed in the case of a cantilever column loaded tangentially at its unsupported end, even though no static buckling load could be found. The critical load for this type of buckling appropriately may be called a "Beck load" P_B in contrast to the more usual "Euler load" P_E that governs bifurcation-type buckling failure.

The concepts involved here are understood readily by the analysis of a simple linked bar system as illustrated in Fig. 2. Two massless bars are linked together and carry point masses of magnitude m at the joint and at the free end. The bars are restrained from free rotation by torsional springs, each of modulus k as shown. The "column" thus formed is compressed by two forces, P that remains directed along the upper link and Q that remains vertical. Equations of motion are

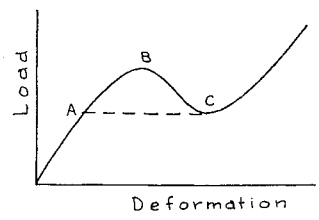

Fig. 1 Shape of load deformation curve.

Received May 10, 1963.

* Professor of Engineering Mechanics, Department of Engineering Mechanics.

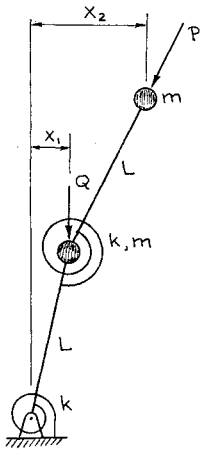

Fig. 2 Analysis of simple linked bar system.

formed easily (assuming small displacements) and are given by Eq. (1):

$$\left[\frac{mL^2}{k}\ddot{X}_1 + \left(1 - \frac{2PL}{k} - \frac{QL}{k}\right)X_1\right] + \left[\frac{2mL^2}{k}\ddot{X}_2 + \frac{PL}{k}X_2\right] = 0 \quad (1)$$

$$[-2X_1] + \left[\frac{mL^2}{k}\ddot{X}_2 + X_2\right] = 0$$

In Eq. (1) dots signify differentiation with respect to time. As usual, one seeks solutions of the form

$$X_i = A_i e^{\lambda t} \quad (2)$$

and finds the characteristic equation of the problem to be

$$\beta^2 + 2\beta\{3 - p[1 + (a/2)]\} + [1 - ap] = 0 \quad (3)$$

where

$$\beta = mL^2\lambda^2/k \qquad p = PL/k \qquad a = Q/P$$

Clearly, for stability of the system, β must be a real number less than zero. Otherwise, at least one root λ will occur which has a positive real part, in which case Eq. (2) indicates unbounded motion. The conditions for β to be a negative real number are

$$(1 - ap) > 0 \quad (4)$$

$$\{3 - p[1 + (a/2)]\}^2 > (1 - ap) \quad (5)$$

$$\{3 - p[1 + (a/2)]\} > 0 \quad (6)$$

The critical state occurs when these inequalities are replaced by equalities. Equation (4) leads to the Euler critical load

$$Q_E = k/L \quad (7)$$

that shows that the system may buckle by ordinary static means. The criteria of Eqs. (5) and (6) are more complex, however, and when violated lead to dynamic buckling in the Beck sense. It is interesting to display these stability boundaries graphically as is done in Fig. 3, where the stable region is shown shaded. Figure 3 will be changed quantitatively by reassigning the mass and stiffness distribution of the "column" but the qualitative features will remain.

In particular it may be noted that if the ratio $Q:P$ is held fixed and of the order of one-quarter, say, the system has both a Beck load P_B and an Euler load P_E, and $P_B < P_E$. If a number of these physical systems were to be built and tested in the laboratory, one should expect to find a scatter of observed buckling loads all the way from P_B to P_E. The value achieved in any particular test would depend on minor details of fit, friction, ambient vibration, etc. This mechanical system is the first one known to the writer which (theoretically at least) exhibits a wide natural experimental scatter.

A theoretical scatter of this type would go far to explain phenomena observed in shell buckling experiments. It would predict not only the wide variation in observed results, but it also would provide a mechanism for the jump from A to C in Fig. 1, which seems to enable a shell to fail at its lower critical load without first passing through its upper critical value. Further, since a nonconservative force, like P in Fig. 2, is necessary for the display of this scatter, the good correlation of theory and experiment in the case of conservative loads also is predicted, as exemplified by the concentrated point load dealt with in Biezeno's analysis.

One must inquire as to the sources of nonconservative forces in real shell buckling problems. Evidently, these will be found in the pressurizing rigs and in the accurate expressions for the fluid pressure forces acting on the shell in the test. Dynamically instrumented tests rarely are reported in the literature, but Ref. 3 indicates that buckles formed on the test shell in question in about 0.006 sec. If this speed of deformation is taken as typical of what may be expected it is clear that the inertia forces both in the fluid medium and in the shell itself may be expected to play an important part. It also can be seen in Ref. 3 that the buckling is not a quasistatic process since the deformation pattern changes during the course of the failure.

In the forementioned column example, the Beck load is a function of the mass distribution as well as of the stiffness distribution. This is a typical result and a distinguishing feature in cases of dynamic buckling. Euler loads on the other hand are independent of mass distribution but do depend on stiffness distribution. If, indeed, a pressurized shell does have a Beck critical load, that load will be alterable by changing the mass distribution on the shell. The experiments designed to detect the presence of this effect should not be difficult to perform.

Yet another effect that ought to be considered in certain cases is the time history of the applied pressure in a test. It well may happen that, if an insufficiently large reservoir is provided and if pressurization is accomplished by a reciprocating pump, the actual pressure on the shell is of the form:

$$P_0 + P_1 \cos\omega t \quad (8)$$

Analysis of a shell with this external loading leads to a Mathieu equation, the solutions of which have well-known stability properties. In particular, an examination of a Strutt diagram shows that even though $P_0 + P_1$ may be removed far from the classical buckling pressure, the shell may yet fail to be dynamically stable so that it will oscillate with ever increasing amplitude. This oscillation would provide the transition to an ultimate collapse mechanism. The shallow spherical cap supported by shear diaphragms over a rectangular planform and loaded by a pressure of the type of Eq. (8) can be analyzed in a straight forward manner, and the associated experiments ought not to be difficult to perform. The spherical cap supported on a circular plan is analytically more diffi-

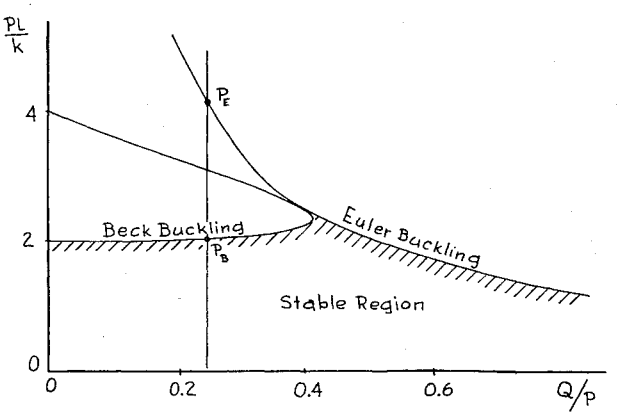

Fig. 3 Stability boundaries.

cult to treat. Oniashvili's book,[6] which makes some attack on problems of dynamically loaded shells, should be mentioned here, although that author's main interest is in the loading through pulsating membrane forces that would be encountered in earthquake resistance studies applied to building structures.

References

[1] Evan-Ivanowski, R. M. and Loo, T. C., "Deformations and stability of spherical shells under action of concentrated loads and uniform pressure," Syracuse Univ. Res. Rept. 834(11), no. 4 (June 1962).

[2] Thurston, G. A., "Comparison of experimental and theoretical buckling pressures for spherical caps," *Collected Papers on Instability of Shell Structures*, NASA TNAD-1510 (1962).

[3] Tennyson, R. C., "A note on the classical buckling load of circular cylindrical shells under axial compression," AIAA J. **1**, 475–476 (1963).

[4] Evan-Ivanowski, R. M., Loo, T. C., and Tierney, D. W., "Local buckling of shells," *Proceedings of the Eighth Midwestern Mechanics Conference* (Pergamon Press, New York, to be published).

[5] Beck, M., "Die Knicklast des einseitig eingespannten, tangential gedrückten Stabes," Z. Angew. Math. Phys. **3**, 225–228 (1952); for a discussion of Beck's work, see Timoshenko, S., and Gere, J. M., *Theory of Elastic Stability* (McGraw-Hill Book Co., New York, 1961), Chap. 2, pp. 152–156.

[6] Oniashvili, O. D., "Certain dynamic problems of the theory of shells," English transl., U. S. Dept. Commerce, Office Tech. Services 62-11592 (1962).

Approximate Analytic Solutions for the Range of a Nonlifting Re-Entry Trajectory

THEODORE R. KORNREICH*

Polytechnic Institute of Brooklyn, Freeport, N. Y.

Nomenclature

A	=	frontal area of re-entry body, ft^2
B_1,B_2,B_3,B_4	=	functions described by Eqs. (17) and (18)
C_1,C_2	=	constants in Eq. (18)
C_D	=	drag coefficient
C_L	=	lift coefficient
g	=	gravitational acceleration, ft/sec^2
h	=	altitude, ft
m	=	mass, slugs
r	=	distance from center of earth to re-entry body, ft
t	=	time, sec
V	=	velocity, fps
x	=	range, ft
β	=	constant in expression for exponential atmosphere 1 ft^{-1}/22,000
θ	=	flight path angle, rad
ρ	=	atmospheric density, slugs/ft^3

Subscripts

c	=	circular, critical
e	=	entry into earth's atmosphere
f	=	condition when $\theta = 90°$
m	=	minimum
s	=	sea level

Received May 20, 1963. The study was supported partially by the Air Force Office of Scientific Research Grant No. AF-AFOSR-1-63. The author wishes to thank Lu Ting for his guidance and encouragement in this work.

* Research Associate, Aerodynamics Laboratory. Member AIAA.

THIS note presents the development of approximate analytic solutions for the evaluation of the range of re-entry trajectories. It is known that, if a body re-enters the atmosphere at subcircular velocity, its trajectory will be of the direct impact type, whereas if the re-entry velocity is supercircular, either a skip or direct impact trajectory will prevail, depending upon the values of re-entry angle and velocity. Therefore, as a prelude to the analysis of the range an investigation was carried out to establish a simple criterion for the determination of whether a given supercircular re-entry trajectory is of the skip or direct impact type.

Wang and Ting[1] presented the following expression applicable to skip trajectories, relating velocity, density, and entry angle:

$$\theta = \left[\theta_e^2 - \frac{C_L A}{m\beta}(\rho - \rho_e) - \frac{2}{\beta}\left(\frac{1}{r} - \frac{g}{V_e^2}\right)\ln\frac{\rho}{\rho_e}\right]^{1/2} \quad (1)$$

where subscript e denotes conditions at entry into the earth's atmosphere. Assuming $C_L = 0$ and evaluating (1) when entry angle reaches its minimum ($\theta = 0$),

$$\ln\frac{\rho_0}{\rho_e} = \frac{\beta\theta_e^2}{2g[(1/V_c^2) - (1/V_e^2)]} \quad (2)$$

where V_c is the orbital velocity at the earth's surface, equal to $(gr)^{1/2}$.

Table 1 Critical angle comparison for various re-entry conditions

V_e/V_c	m/C_DA, slugs/ft^2	θ_c, rad (analytic approx.)	θ_c, rad (machine calculation)
1.2	1.94	0.076	0.073
1.2	0.40	0.071	0.068
1.2	10.0	0.090	0.084
1.37[a]	1.94	0.153	0.149
1.4	1.94	0.108	0.099
1.7	1.94	0.128	0.119
1.7[a]	1.94	0.185	0.180

[a] These correspond to atmospheric entry altitude of 660,000 ft. Other cases were evaluated at 400,000 ft.

In the case of direct impact re-entry trajectories, the relationship of Allen and Eggers[2] may be used to calculate the density ρ^* corresponding to a prescribed set of re-entry conditions:

$$\rho^* - \rho_e = \frac{2m\beta\sin\theta_e}{C_DA}\ln\frac{V_e}{V} \quad (3)$$

For a prescribed supercircular re-entry velocity, it is of interest to determine the critical entry angle at which a trajectory switches from the direct impact to the skip type. When $V_e > V_c$, the value of θ_e decreases, reaches a minimum (corresponding to $V = V_c$), as seen from the equation of motion for $d\theta/dt$, and then increases once again. Therefore, a comparison of ρ^* and ρ_0 will indicate the type of trajectory to be expected for any given case, i.e., $\rho^* > \rho_0$ indicates skip trajectory; $\rho_0 > \rho^*$ indicates direct impact trajectory; and $\rho_0 = \rho^*$ specifies the critical entry angle.

The following iterative procedure may be used to determine θ_e: assume a value for θ_e and calculate ρ^* from Eq. (3). Use this value of ρ^* as a trial value for ρ_0 and calculate the corresponding θ_e from Eq. (2). If the assumed and calculated values of θ_e do not agree within tolerable limits, use the calculated value as the new trial value for θ_e and iterate once more. A rapid convergence toward the correct value will be obtained since the value of ρ^* varies little within a reasonably wide spread of values of entry angle.